Safety and Preliminary Efficacy of Pembrolizumab Following Transarterial Chemoembolization for Hepatocellular Carcinoma: The PETAL Phase Ib Study

David J. Pinato[1,2], Antonio D'Alessio[1,2], Claudia Angela Maria Fulgenzi[1], Alexandra Emilia Schlaak[3], Ciro Celsa[1,4], Saskia Killmer[3], Jesus Miguens Blanco[5], Caroline Ward[1], Charalampos-Vlasios Stikas[1], Mark R. Openshaw[6], Nicole Acuti[1], Georgios Nteliopoulos[1], Cristina Balcells[1], Hector C. Keun[1], Robert D. Goldin[7], Paul J. Ross[8,9], Alessio Cortellini[1,10], Robert Thomas[11], Anna-Mary Young[12], Nathan Danckert[5], Paul Tait[11], Julian R. Marchesi[5], Bertram Bengsch[3,13,14], and Rohini Sharma[1]

ABSTRACT

Purpose: Transarterial chemoembolization (TACE) may prime adaptive immunity and enhance immunotherapy efficacy. PETAL evaluated safety, preliminary activity of TACE plus pembrolizumab and explored mechanisms of efficacy.

Patients and Methods: Patients with liver-confined hepatocellular carcinoma (HCC) were planned to receive up to two rounds of TACE followed by pembrolizumab 200 mg every 21 days commencing 30 days post-TACE until disease progression or unacceptable toxicity for up to 1 year. Primary endpoint was safety, with assessment window of 21 days from pembrolizumab initiation. Secondary endpoints included progression-free survival (PFS) and evaluation of tumor and host determinants of response.

Results: Fifteen patients were included in the safety and efficacy population: 73% had nonviral cirrhosis; median age was 72 years. Child-Pugh class was A in 14 patients. Median tumor size was 4 cm. Ten patients (67%) received pembrolizumab after one TACE; 5 patients after two (33%). Pembrolizumab yielded no synergistic toxicity nor dose-limiting toxicities post-TACE. Treatment-related adverse events occurred in 93% of patients, most commonly skin rash (40%), fatigue, and diarrhea (27%). After a median follow-up of 38.5 months, objective response rate 12 weeks post-TACE was 53%. PFS rate at 12 weeks was 93% and median PFS was 8.95 months [95% confidence interval (CI): 7.30–NE (not estimable)]. Median duration of response was 7.3 months (95% CI: 6.3–8.3). Median overall survival was 33.5 months (95% CI: 11.6–NE). Dynamic changes in peripheral T-cell subsets, circulating tumor DNA, serum metabolites, and in stool bacterial profiles highlight potential mechanisms of action of multimodal therapy.

Conclusions: TACE plus pembrolizumab was tolerable with no evidence of synergistic toxicity, encouraging further clinical development of immunotherapy alongside TACE.

Introduction

Patients presenting with liver-confined hepatocellular carcinoma (HCC), preserved liver function, and good performance status cluster into "intermediate stage" or Barcelona clinic liver cancer (BCLC) B stage (1). In this patient subgroup, where overall survival (OS) often extends beyond 2 years, guidelines recommend transarterial chemoembolization (TACE) with the intent of prolonging OS by achieving local tumor control and prevent systemic spread of the disease (2).

The efficacy of TACE relies on the dual ischemic and cytotoxic effect stemming from the sequential intra-arterial delivery of cytotoxic chemotherapy followed by direct occlusion of the arterial neovascular supply to the tumor. Clinically, this translates into radiologically measured responses in 35% of patients, which associates with a 14% improvement of patients' survival at 2 years (3). While the therapeutic landscape of advanced HCC has recognized a number of advancements, management of BCLC B HCC has marginally shifted due to demonstration of benefit of TACE over placebo in the early 2000s (4). While combination of TACE with sorafenib might counteract tumor progression in selected patients (5), the lack of a convincing OS benefit (6, 7) in association with synergistic toxicity seen

[1]Department of Surgery and Cancer, Faculty of Medicine, Imperial College London, Hammersmith Hospital, London, United Kingdom. [2]Division of Oncology, Department of Translational Medicine, University of Piemonte Orientale, Novara, Italy. [3]Department of Internal Medicine, University Hospital Freiburg, Freiburg, Germany. [4]Section of Gastroenterology and Hepatology, Department of Health Promotion, Mother and Child Care, Internal Medicine and Medical Specialties, PROMISE, University of Palermo, Palermo, Italy. [5]Department of Metabolism, Digestion and Reproduction, Faculty of Medicine, Imperial College London, St Mary's Hospital Campus, London, United Kingdom. [6]Institute of Cancer and Genomics Sciences, University of Birmingham, Birmingham, United Kingdom. [7]Centre for Pathology, Imperial College London, Charing Cross Hospital, London, United Kingdom. [8]Department of Medical Oncology, Guy's and St Thomas' NHS Foundation Trust, London, United Kingdom. [9]King's College Hospital NHS Foundation Trust, London, United Kingdom. [10]Division of Medical Oncology, Policlinico Universitario Campus Bio-Medico, Rome, Italy. [11]Interventional Radiology, Imperial College NHS Trust, Hammersmith Hospital, London, United Kingdom. [12]Department of Medical Oncology, St Georges University Hospitals, NHS Foundation Trust, St George's University Hospitals NHS Foundation Trust, London, United Kingdom. [13]Signalling Research Centres BIOSS and CIBSS, University of Freiburg, Freiburg, Germany. [14]German Cancer Consortium (DKTK), Heidelberg, Germany, partner site Freiburg.

D.J. Pinato, A. D'Alessio, C.A.M. Fulgenzi, and A.E. Schlaak contributed equally as co-first authors and B. Bengsch and R. Sharma as co-senior authors to this article.

Corresponding Author: David J. Pinato, Imperial College London, Hammersmith Campus, London W12 0HS, United Kingdom. E-mail: david.pinato@imperial.ac.uk

Clin Cancer Res 2024;30:1–11

doi: 10.1158/1078-0432.CCR-24-0177

Translational Relevance

PETAL is the first early-phase clinical trial testing the hypothesis of synergy between transarterial chemoembolization (TACE) and sequential PD-1–targeted immunotherapy for liver-confined hepatocellular carcinoma (HCC). With the growing interest in the use of immune checkpoint inhibitors (ICI) in the early stages for HCC, PETAL confirms the feasibility of the combined approach between ICI and locoregional treatments, supporting their ongoing investigation in larger, randomized phase III trials.

from combination of certain antiangiogenics with TACE (8) calls for the development of novel therapeutic combinations to improve patient outcomes in this highly heterogeneous stage of HCC. Immune checkpoint inhibitors (ICI) targeting the programmed-cell death 1 (PD-1) pathway are effective in a proportion of patients with HCC and now constitute a global standard of care for the treatment of unresectable/advanced HCC, having been demonstrated noninferior to sorafenib as monotherapy in certain trials or superior when administered in association with VEGF targeting antibodies or with CTL antigen-4 (CTLA-4; ref. 9).

The demonstrated efficacy of ICI in advanced HCC has placed increasing emphasis on the immune-modulatory role of locoregional therapies for HCC (10–13). Innate and adaptive immune activation are key prognostic determinants in patients undergoing locoregional therapies including TACE, with chronic modulation of the T-helper-2 lymphocyte response (10, 14–16) and regulatory T cells (17) being associated with clinical outcome after successful local treatment.

The clinical hypothesis underlying this early-phase clinical study is that TACE may act as a locoregional inducer of immunogenic cell death, enabling sequential treatment with the anti-PD-1 antibody pembrolizumab to promote effective immune reconstitution and improve antitumor control. This study aims to characterize safety, preliminary efficacy of TACE plus pembrolizumab, and to explore mechanisms of efficacy using multiple validated readouts of host immunity.

Patients and Methods

Study design and participants

PETAL is a prospective, open-label, single-arm phase Ib trial of pembrolizumab in combination with TACE in patients with liver-confined HCC. The study protocol has been published previously (18). This trial was conducted at tertiary referral centres for the care of HCC (Imperial College, King's College and St. George's Hospital) in London, United Kingdom. Eligible patients were aged ≥18 years, had confirmed radiologic diagnosis of HCC based on the American Association for the Study of Liver Diseases criteria (19), were ineligible for liver resection, transplantation, and were naïve to systemic therapy. At screening, patients were required to have at least one previously untreated lesion (i.e., the TACE-amenable lesion) measurable by RECIST v1.1, an Eastern Cooperative Oncology Group performance status (ECOG PS) of 0–1, adequate organ function (hematology, coagulation, blood chemistry, and hepatorenal function), and a Child-Pugh (CP) class score ≤7. Patients with extrahepatic metastases, hepatic encephalopathy, diuretic-refractory ascites, or history of bleeding were excluded. Full inclusion/exclusion criteria and representativeness of study population are listed in Supplementary Tables S1 and S2.

The study was conducted in accordance with Good Clinical Practice and the Declarations of Helsinki and Istanbul. Study protocol and subsequent amendments were approved by the London Westminster Research Ethics Committee (Reference 17/LO/1180, EudraCT 2017-000471-85, NCT03397654) and the UK Health Research Authority. All patients provided written informed consent prior to participation.

Study procedures

PETAL was conducted in two parts. Study part 1 consisted of a safety run-in of up to 6 participants treated with pembrolizumab administered intravenously over 30 minutes at the dose of 200 mg every 3 weeks at the predefined interval of 30 days (+3 days) post-TACE. Subjects in part 1 were observed for determination of dose-limiting toxicities (DLT), with a particular focus on the emergence of any liver-related adverse events (AE) defined as per system-organ class designation occurring over a 21 days' time window from cycle 1 of pembrolizumab, with weekly laboratory assessments in cycle 1 only. All patients in study part 1 received conventional superselective TACE, consisting of intra-arterial injection of lipiodol plus doxorubicin (60 mg fixed dose) followed by injection of an embolic agent (gelfoam) to arrest blood flow to the tumor. Following completion of part 1 and upon confirmation of safety of the conventional (c) TACE/pembrolizumab combination, patients in part 2 were allowed to have either cTACE or drug eluting beads (DEB) TACE with up to 300–500 μm LC Beads mixed with 150 mg of doxorubicin. Patients achieving incomplete devascularization 4 weeks after initial TACE were considered for a second procedure by treating investigators. Patients requiring >1 TACE were mandated to receive the same type of procedure (either cTACE or cTACE/DEB-TACE if in part 2) and be reassessed for response beginning 4 weeks after second TACE and commence pembrolizumab thereafter. However, after completion of two TACE procedures, all patients who remained eligible by clinical and laboratory features were dosed with pembrolizumab not earlier than 30 days (+3) from the second procedure irrespective of radiologic response to TACE. Tumor reassessments were planned with dynamic CT or MRI 4 weeks after each TACE procedure and subsequently after four cycles of pembrolizumab and continuing every 12 weeks thereafter until end of study. Pembrolizumab was continued until oncological disease progression, unacceptable toxicity, or completion of 1 year of treatment. **Figure 1A** highlights the study flow chart.

Outcomes

The primary study endpoint was to assess safety and tolerability of pembrolizumab following TACE and to determine whether pembrolizumab following TACE could lead to DLT events. Safety assessments included physical and laboratory findings and AEs were defined according to the NCI Common Toxicity Criteria for Adverse Events version 4.0. Patients were assessed for the emergence of AEs before starting immunotherapy (within 30 days after TACE for the first part and within 45 days after TACE in part 2) and then every week for the first 21 days and every 3 weeks thereafter for part 1; for part 2, they were assessed every 3 weeks from cycle 1. The causality between AEs and treatment was assigned by the investigators. Patients were assessed for the emergence of AEs up to 30 days after end of treatment (EOT). A DLT was defined as a treatment-related ≥grade 3 AE occurring during the assessment window of 21 days from the first administration of pembrolizumab. With safety being primary study endpoint, no power calculation for hypothesis testing was required to formally power the

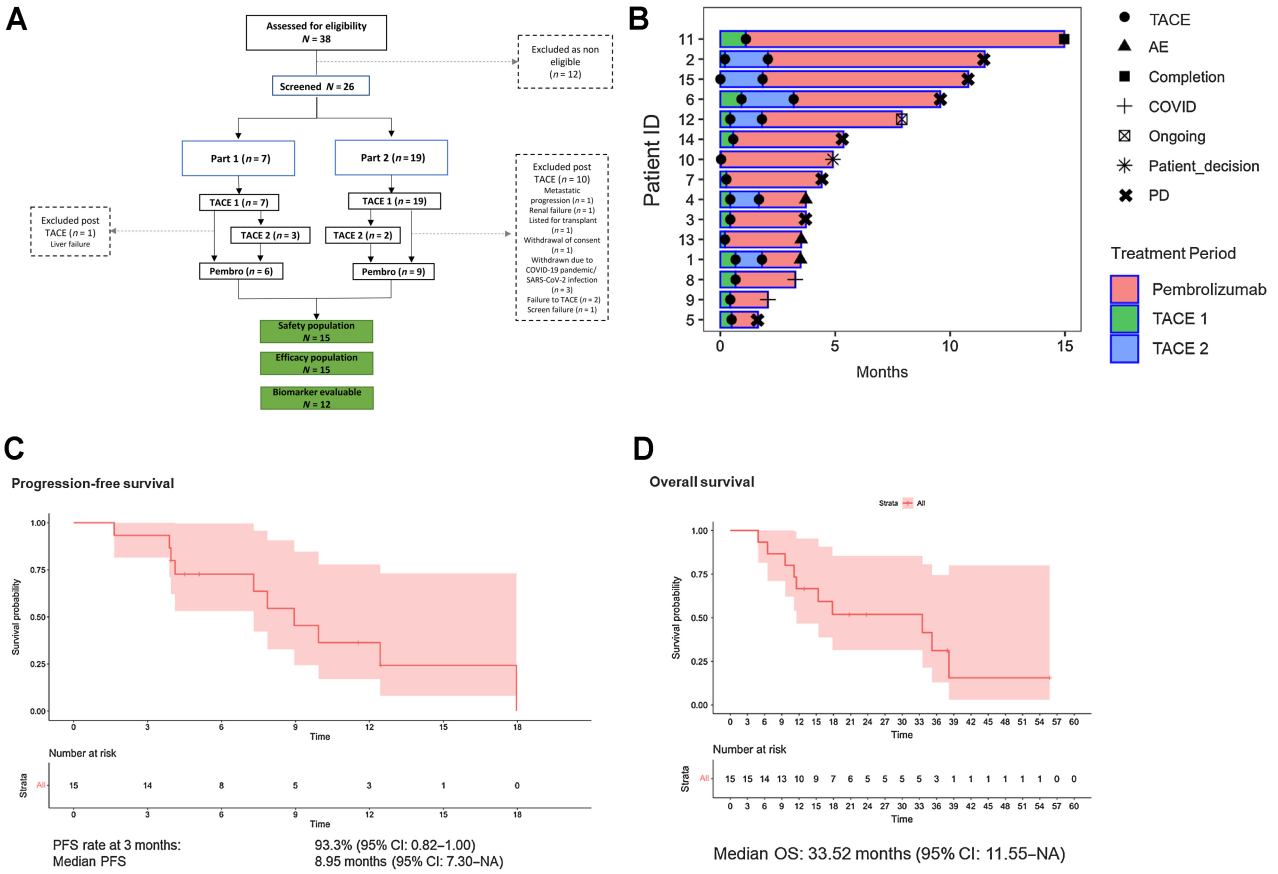

Figure 1.

A, Study flow chart. **B,** Swimmer's plot of study participants receiving TACE plus pembrolizumab. Each bar represents one subject in the study. Depth, duration of response, dates of radiologic response or progressive disease, and presence of ongoing response are indicated accordingly. **C,** Kaplan–Meier curve illustrating the PFS of the study population. **D,** Kaplan–Meier curve illustrating the OS of the study population.

study and the upper 95% confidence interval (CI) for toxicity events was used to inform the decision to proceed to a subsequent efficacy study. Alongside primary safety analyses, an exploratory analysis was performed to obtain preliminary data on the efficacy of the TACE plus pembrolizumab combination. Tumor response was assessed using RECIST v1.1 criteria at screening, 4 weeks after each TACE procedure and every 12 weeks during pembrolizumab treatment. To capture the combined efficacy ot TACE plus pembrolizumab we elected as primary efficacy outcomes the evaluating radiological overall response rates (ORR) at 12 weeks after last TACE, alongside progression-free survival (PFS) and OS.

ORR was defined as the percentage of patients reporting either partial response (PR) or complete response (CR) at the first scan at 12 weeks after the last TACE. Median duration of response was defined as the time from first CR or pathologic response (PR) to death or progression in those achieving an objective response.

PFS was defined by the time from last TACE to the first occurrence of documented disease progression based on RECIST v1.1 criteria or death from any cause, whichever occurred first, and it was calculated using Kaplan–Meier. A PFS rate at 12 weeks was calculated as the percentage of patients free from death or progression at 12 weeks from last TACE using the Kaplan–Meier method. OS was defined from the time of last TACE until death from any cause. PFS was censored at the time of last tumor assessment in those patients who had not progressed by the time of database lock, whereas OS was censored at the time of last patient contact. Survival follow-up was carried out every 8 weeks after EOT. Median follow-up was calculated using reverse Kaplan–Meier method from screening to last follow-up. All patients who received at least one dose of pembrolizumab were included in the safety and efficacy analyses.

Quality-of-life measures

Health-related quality of life (QoL) was evaluated using the European Organisation for Research and Treatment of Cancer (EORTC) Quality-of-life Questionnaire Core 30 (QLQ-C30) and the EORTC Quality-of-life Questionnaire-Hepatocellular Carcinoma 18 (QLQ-HCC18; ref. 20). Further details are reported in Supplementary Data S1.

Biomarker assessments

The comprehensive translational program included analyses on circulating tumor DNA (ctDNA; Supplementary Figs. S1 and S2), peripheral T-cell repertoire, peripheral immune population phenotyping with mass cytometry (Supplementary Fig. S3; Supplementary Tables S3 and S4), targeted transcriptomics on bulk RNA extracted from screening biopsies, stool metataxonomics, and serum metabolomic profiling (Supplementary Table S5). The detailed methods can be found in Supplementary Data S2–S9.

Statistical analyses

Statistical analyses were performed using SPSS version 25.0 (IBM Inc.) and GraphPad PRISM (GraphPad software Inc.) unless stated otherwise, with all estimates being reported with corresponding 95% CIs and a two-tailed level of significance of $P < 0.05$.

Ethics approval and consent to participate

Study protocol and subsequent amendments were approved by the London Westminster Research Ethics Committee (Reference 17/LO/1180, EudraCT 2017-000471-85, NCT03397654) and the UK Health Research Authority. All patients provided written informed consent prior to participation to the study.

Data availability

The data generated in this study are available upon request from the corresponding author. The sequencing data are not publicly available due to patient privacy requirements but are available upon reasonable request from the corresponding author.

Results

Patient characteristics

Patient allocation is highlighted in **Fig. 1A**. From February 2018 to September 2022, 26 patients provided consent and were screened for the study. At the time of database lock (February 28, 2023), 15 patients had received at least one dose of pembrolizumab and completed the DLT period. Patient features at screening are presented in **Table 1**. Median age of the safety-evaluable population was 72 years [interquartile range (IQR): 63.5–75.5], most of the patients were male (73.3%), had liver cirrhosis (73.3%) of nonviral origin (73.4%), and an ECOG performance status of 0 (60.0%). One patient with CP B liver class was enrolled in the safety run-in phase, and the remaining scored A (66.6% CP 5 and 26.6% CP 6). All patients had liver-confined HCC; the majority had one single neoplastic nodule (53.3%), with a median maximum tumor diameter of 4 cm (IQR: 3.4–4.5). Most patients were treatment-naïve for HCC, with only 1 patient (9%) having received prior radiofrequency ablation to an unrelated lesion.

Table 1. Baseline characteristic of the safety-evaluable population.

Age, median (IQR)	72 (63.5–75.5)
Gender, *n* (%)	
Male	11 (73.3%)
Female	4 (26.7%)
Ethnicity, *n* (%)	
White	8 (53.3%)
Asian	2 (13.3%)
Other (not stated)	5 (33.4%)
ECOG PS, *n* (%)	
0	9 (60.0%)
1	6 (40.0%)
AFP (ng/mL), median (IQR)	16 (6.5–37.5)
Child Pugh, *n* (%)	
5	10 (66.6%)
6	4 (26.6%)
7	1 (6.8%)
ALBI, *n* (%)	
1	6 (40.0%)
2	9 (60.0%)
Cirrhosis, *n* (%)	
Present	11 (73.3%)
Absent	4 (26.7%)
Etiology, *n* (%)	
Viral	4 (26.6%)
Nonviral	11 (73.4%)
HBV	2 (13.3%)
HCV	2 (13.3%)
BCLC, *n* (%)	
A	7 (46.6%)
B	8 (53.4%)
Number of nodules, *n* (%)	
1	8 (53.3%)
2	3 (20%)
3	4 (26.7%)
Maximum diameter (cm), median (IQR)	4 (3.4–4.5)
Previous surgery, *n* (%)	
Yes	0
No	0
Previous RFA, *n* (%)	
Yes	2 (13.3%)
No	13 (86.7%)
Previous TACE, *n* (%)	
Yes	1 (6.6%)
No	14 (93.4%)

Safety and QoL

In the 6 patients enrolled in study part 1, no DLTs were observed from the combination of TACE with pembrolizumab in the 21 days following first pembrolizumab administration. One patient who commenced treatment with CP B7 functional class discontinued treatment after completion of DLT window due to treatment-unrelated worsening of liver functional reserve (grade 1 bilirubin increase from baseline and grade 2 ascites). Following the independent data safety monitoring committee review, the protocol was amended to continue recruitment to CP A disease patients only.

Throughout the observation period, 14 patients (93.3%) developed at least one AE of any grade, and 7 (46.7%) grade 3 or higher. No grade 4 or 5 AEs were reported. As described in **Table 2**, fatigue and anorexia were the most reported AEs, occurring in 10 participants (66.7%), followed by skin rash (60.0%) and diarrhea (53.3%). Fourteen patients (93.3%) experienced at least one treatment-related AE (TRAE) of any grade. Skin rash was the most common TRAE (40.0%), followed by diarrhea, pruritus, and fatigue occurring in 4 participants each (26.7%; Supplementary Table S6). The only grade 3 TRAE reported, skin rash (6.7%), required oral corticosteroid treatment and subsequently resolved allowing treatment resumption. Sequential administration of pembrolizumab after TACE did not result in unexpected hepatic toxicity as supported by longitudinal liver function tests (Supplementary Fig. S4).

Mean scores for global health status (GHS)/QOL and functioning domains on EORTC QLQ-C30 questionnaire and for symptom scales on EORTC QLQ-C30 and QLQ-HCC18 questionnaires at baseline and at the EOT are reported in Supplementary Table S7 and Supplementary Figs. S5 and S6, showing a favorable trend in most domains. Mean changes from baseline in GHS/QoL and functioning domains are showed in Supplementary Fig. S7.

Efficacy

At data cutoff, 15 patients were evaluable for efficacy: 10 (66.7%) had received one round of TACE, whereas 5 (33.3%) had required two procedures prior to starting immunotherapy. Tumor assessment performed 4 weeks after TACE and before pembrolizumab initiation demonstrated that 6 patients achieved CR to TACE (40%), 2 had a PR

Table 2. All-cause AEs occurring in ≥15% of the safety-evaluable population.

Adverse event	Any grade *N* (%)	Grade ≥3 *N* (%)
All	14 (93.3%)	7 (46.7%)
Fatigue	10 (66.7%)	1 (6.7%)
Anorexia	10 (66.7%)	1 (6.7%)
Skin rash	9 (60.0%)	1 (6.7%)
Diarrhea	8 (53.3%)	1 (6.7%)
Dyspnea	6 (40.0%)	None
Back pain	6 (40.0%)	None
Pruritus	5 (33.3%)	None
Lethargy	5 (33.3%)	None
Abdominal distension	5 (33.3%)	None
Dry mouth	5 (33.3%)	None
Peripheral edema	5 (33.3%)	None
Peripheral neuropathy	5 (33.3%)	None
Abdominal pain	4 (26.67%)	1 (6.7%)
Flu-like symptoms	4 (26.67%)	1 (6.7%)
Cough	4 (26.7%)	None
Nausea	4 (26.7%)	None
Bilirubin increase	3 (20.0%)	1 (6.7%)
Mucositis	3 (20.0%)	None
Dysgeusia	3 (20.0%)	None
Hypothyroidism	3 (20.0%)	None
Upper respiratory infection	3 (20.0%)	None

(13.3%), and 7 patients (46.7%) achieved radiological stable disease as best response to TACE.

Pembrolizumab was commenced in all patients at least 30 (+3) days after TACE (median 1.05 months, IQR: 1.00–1.35). Median duration of pembrolizumab treatment was 3.1 months (IQR: 1.5–5.1) and median number of administered cycles was 5 (IQR: 3.0–7.5).

After a median follow-up of 38.5 months (95% CI: 24.7–52.5), all 15 patients had stopped immunotherapy. Radiologically proven disease progression was the most common cause of pembrolizumab cessation occurring in 7 (46.7%) subjects, after a median of 5 cycles (IQR: 3.0–6.8). Other causes for premature pembrolizumab discontinuation included treatment-unrelated progression of liver dysfunction ($n = 2$), grade 3 diarrhea secondary to *Clostridium difficile* infection ($n = 1$), treatment-related persisting grade 2 peripheral neuropathy ($n = 1$), COVID-19 pandemic ($n = 2$), and withdrawal of consent ($n = 1$). A Swimmer's plot summarizing these events and their timing is showed in **Fig. 1B**.

At the time of data cutoff, the PFS rate at 12 weeks from the last TACE was 93.3% (95% CI: 0.82–1.00), and median PFS from last TACE was 8.95 months [95% CI: 7.30–NE (not estimable); **Fig. 1C**]. ORR at 12 weeks from last TACE was 53.3% and included 2 PR and 6 CR. Median duration of response was 7.3 months (95% CI: 6.3–8.3). By the time of data cutoff, 10 patients had died, with a median OS of 33.5 months (95% CI: 11.5–NE) from enrollment. The 6-month and 1-year OS rates were 93.3% (95% CI: 0.82–1.00) and 70% (0.49–0.99), respectively (**Fig. 1D**).

ctDNA and T-cell receptor repertoire

We performed a tumor-informed ctDNA analysis using a bespoke panel validated by our group (21) in all patients with quantifiable cell-free (cfDNA) in peripheral plasma in at least one timepoint. We sequenced the cfDNA extracted from a total of 28 timepoints, and 10 patients were considered eligible, of whom 4 achieved a radiological response at 12 weeks (40%).

Baseline characteristics are summarized in Supplementary Table S8. At screening, cfDNA was detectable at the median concentration of 0.57 ng/μL (IQR: 0.46–0.72), of which ctDNA accounted for a median of 8.5% (IQR: 4.2–17.6). While cfDNA at screening did not differ across responders and nonresponders (median 0.73 vs. 0.57 ng/μL, $P = 0.25$), baseline ctDNA was significantly higher in responders (median 0.15 vs. 0.06 ng/μL, $P = 0.01$; **Fig. 2A**).

When longitudinally analyzing ctDNA across timepoints, we observed that the radiological response was recapitulated by the evolution of ctDNA concentration. In fact, ctDNA concentration significantly decreased during ICI treatment in responders (median 0.15 vs. 0.07 ng/μL at screening and on treatment, respectively, $P = 0.0048$), while a significant increase was observed in nonresponders from screening to EOT (median 0.06 vs. 0.08 ng/μL, $P = 0.003$; **Fig. 2A**).

Most frequent mutated gene was *ARID1A* (41% of samples), followed by *PI3KCA* (33%) and *HNF1A* (22%; **Fig. 2B** and **C**). For patients with an available paired assessment, the variant allele frequency (VAF) of ARID1A appeared to dynamically follow the course of the treatment, with a decrease on-treatment and an increase upon treatment failure (Supplementary Fig. S8A). Both in samples of responders and nonresponders, the VAF of specific variants mirrored the evolution of the treatment, with a clearance after TACE and an increase at treatment failure (Supplementary Fig. S8B and S8C).

We investigated whether the TCRb repertoire underwent any modifications across the different timepoints, and whether it was associated with the achievement of radiological response at 12 weeks. We found that TACE did not significantly impact on clonality, even after subdividing per response (Supplementary Fig. S9A–S9C), and we did not find any significant change in clonality induced by ICI administration (Supplementary Fig. S9D–S9F). However, when looking at the TCRb repertoire prior to ICI commencement, we observed a significantly higher productive Simpson clonality in responders, as also shown by the frequency of the top 10 rearrangements (**Fig. 2D** and **E**), with no difference in entropy (Supplementary Fig. S10A and S10B).

Peripheral immune phenotyping

We used highly multiplexed mass cytometry (CyTOF) for immune monitoring and longitudinal phenotyping of peripheral blood mononuclear cells isolated at multiple timepoints: screening (i.e., pre-TACE), pre-pembrolizumab, at cycle 5 of pembrolizumab, and at the EOT. In total, 13 out of 15 patients were evaluable for analysis. Data analysis was performed on the basis of gating of $n = 30$ predefined immune cell populations (Supplementary Fig. S3) and via an unbiased data-driven clustering pipeline.

We investigated dynamic changes of immune cell subpopulations along the study, and we correlated the findings with the achievement of radiological response after 12 weeks, in keeping with the secondary clinical endpoint. Interestingly, when comparing the immune subpopulations at screening and at treatment discontinuation, we observed a significant enrichment in $CD8^+$ $CXCR5^-CCR4^+CXCR3^-CCR6^-$Tc2 at EOT compared with baseline (**Fig. 3A** and **B**). Screening for possible predictors of immunotherapy response, we observed that $CD8^+$ $CXCR5^-CCR4^-CXCR3^+CCR6^-$ Tc1 cells were significantly more represented in nonresponders compared with responders prior to ICI initiation (**Fig. 3C**). At the EOT, a significant increase in $CD3^-CD19^+$ B cells was observed in nonresponders (**Fig. 3D**). In summary, while overall the data indicate limited variation in the broad immune profile, individual immune cell subsets were linked to treatment efficacy.

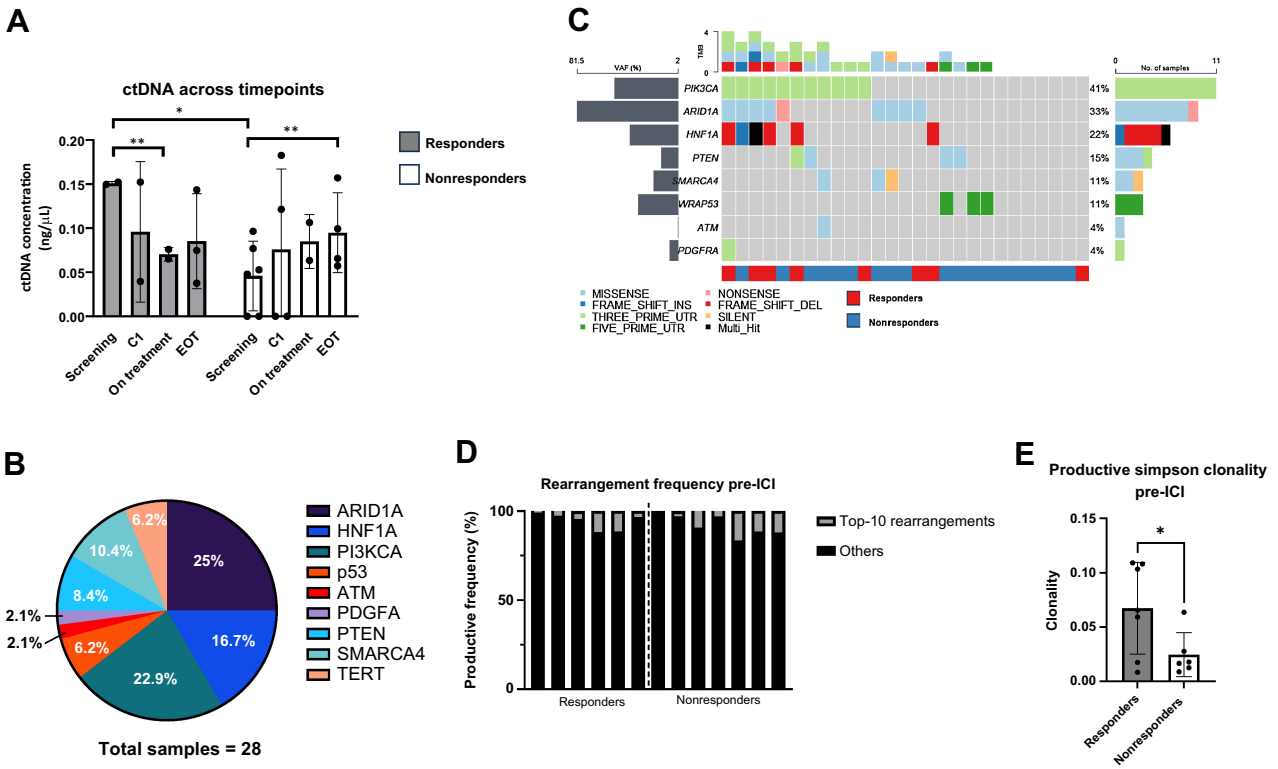

Figure 2.

A, Dynamic changes of ctDNA concentration at various study timepoints and relationship with response to treatment. **B,** Distribution of individual mutations across pretreatment samples ($n = 28$). **C,** Oncoplot illustrating the distribution and type of mutations identified in pretreatment plasma samples of patients recruited to the study. Each column represents a sample and each row a different gene. The left barplot illustrates the VAF pertaining to each sample, while the right barplot has the frequency of mutations in each gene. The top bar plot estimates the tumor mutational burden (TMB) calculated on the basis of number of mutations per megabase of sequenced genome. Samples are ordered by the most mutated genes. **D,** Distribution of the top 10 T-cell receptor rearrangements as measured by productive frequency prior to pembrolizumab start in responders ($n = 6$) and nonresponders ($n = 7$; $n = 2$ not available). **E,** Productive Simpson clonality was significantly higher in responders before commencement of systemic therapy. *, $P < 0.05$; **, $P < 0.01$.

We thus focused our analysis on the heterogeneity of T-cell responses using a data-driven high-dimensional clustering approach. $CD45^+CD3^+CD19^-$ T cells were sampled from nonresponder and responder patients and the T-cell landscape was visualized using t-distributed stochastic neighbor embedding (tSNE) dimension reduction (**Fig. 4A**). As expected, Tc1 and Tc2 cells identified as differentially expressed in our prior predefined analysis also differed in their localization on the T-cell map in areas associated with different outcomes (**Fig. 4B** and **C**). Our data-driven clustering approach further revealed 12 distinct subsets of T cells in the patient cohort (**Fig. 4D**). Notably, two T-cell subsets prior to ICI therapy, cluster c07 and cluster c08, were associated with differential patient outcomes: cluster c08 was enriched in patients who responded to therapy, while cluster c07 was enriched in nonresponders (**Fig. 4E**). Phenotypic analysis informed c07 as an early differentiated memory $CD4^+$ T-cell cluster, whereas c08 represented a Th1-like CD4 T-cell cluster with high levels of T-bet, CX3CR1, KLRG1, and CD57 (**Fig. 4F**). These data suggest that the presence of a Th1-polarized T-cell response prior to anti-PD-1 checkpoint therapy is associated with the achievement of response to treatment.

Targeted transcriptomics of baseline tumor biopsies

We performed bulk targeted transcriptomic analyses on total RNA purified from 10 pretreatment biopsies obtained at screening that satisfied quality control criteria. In exploratory analyses, we compared differences in the expression of 770 genes related to adaptive and innate immunity (NanoString Pancancer Immune panel) in 4 responders and 6 nonresponders (Supplementary Fig. S11A). Samples from patients achieving a response to TACE plus pembrolizumab were enriched for gene expression signatures reflective of innate immunity including cytokine and chemokine secretion and regulation of macrophage function (Supplementary Fig. S11B). Differential gene expression analysis highlighted transcripts involved in the inflammatory process such as *FN1*, *SPP1*, and *LBP* (Supplementary Fig. S12A and S12B).

Stool bacterial profiles and metabolic phenotyping

The microbiota-evaluable population consisted of 9 patients, with available paired stool samples. After filtering for the presence of adequate count of sequencing reads, we included 6 patients, whose baseline characteristics can be found in Supplementary Table S9. The most prevalent genus at baseline was *Bacteroides* (Supplementary Fig. S13), with no significant changes in alpha and beta diversity measures across screening and EOT timepoints (Supplementary Fig. S14A–S14D). We identified a significant enrichment in the *Clostridium* genus in stool samples at screening, while *Alistipes* was found to be significantly increased at treatment discontinuation (Supplementary Fig. S14E).

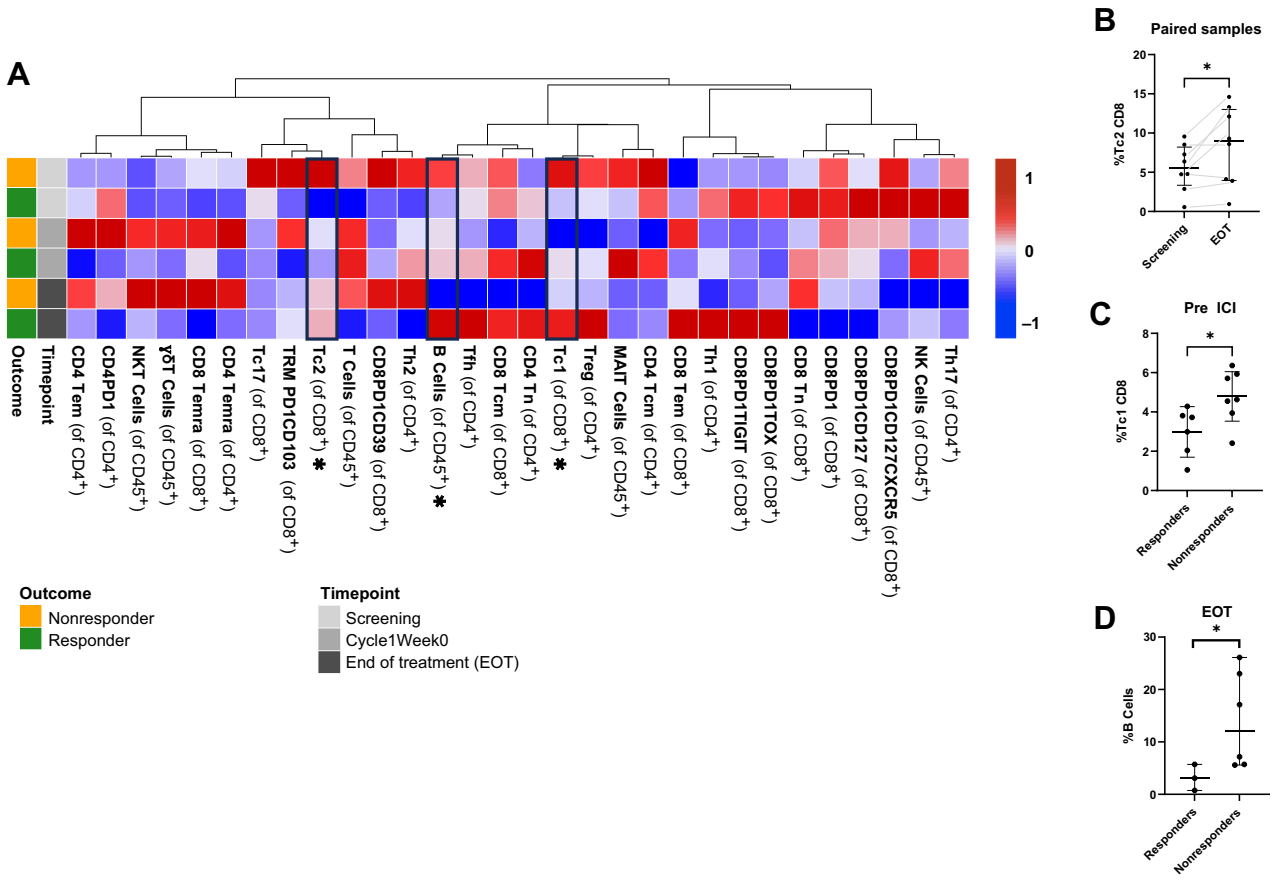

Figure 3.

A, Heat map illustrating relative representation of individual cell types as assayed using CyToF across the various study timepoints (screening, cycle 1 week 0, that is, post-TACE, and EOT) stratified on the basis of the achievement of response 12 weeks following TACE plus pembrolizumab combination. Hierarchically clustered heat map displays mean frequencies of lymphocyte subsets per timepoint and response to therapy, visualized by z-score–based coloring after column normalization. **B,** Tc2 cell frequency differed between screening and EOT ($n = 8$, paired samples). **C,** Tc1 cell frequency before ICI therapy was different between responders ($n = 6$) and nonresponders ($n = 7$). **D,** B-cell frequency differed at end of therapy between responders ($n = 6$) and nonresponders ($n = 7$). *, $P < 0.05$.

We included in the metabolomics analysis 23 serum samples, collected from 11 patients at three different timepoints: at screening (prior to TACE), prior to pembrolizumab commencement (C1W0), and at the EOT. Baseline characteristics of these patients can be found in Supplementary Table S10. When comparing samples collected at screening and at EOT, we found a significant higher abundance of several acylcarnitines at screening, while the ratio of tyrosine/phenylalanine was significantly increased at the EOT (Supplementary Fig. S15A).

Data on response to treatment at 12 weeks were available for 8 patients. Sera of responders was found to be significantly enriched in two acylcarnitines and four phosphatidylcholine lipids (PCaa), while the ratio of methionine-sulfoxide/methionine and the ratio of total acylcarnitine derivatives of dicarboxylic acids (AC-DC)/total acylcarnitines were significantly increased in nonresponders (Supplementary Fig. S15B).

Discussion

It has been recognized for a long time that local therapy may evoke significant immunologic consequences in patients with HCC. Local and systemic secretion of proinflammatory cytokines and danger-associated molecular patterns following successful tumor chemoembolization has a priming effect on adaptive immunity (22). Patients who mount a spontaneous CD4 and CD8 response following TACE exhibit improved survival outcomes, underscoring immune modulation as a fundamental mechanism underlying the efficacy of TACE (10, 14–16). Therapeutic combinations between locoregional and systemic immunotherapies are at the focus of intense research efforts (23).

In this phase Ib study, the combination of TACE plus pembrolizumab was well tolerated and did not lead to synergistic toxicity or unexpected safety concerns. Most TRAEs were grade 1 or 2 and entirely attributable to pembrolizumab exposure with rates and intensity of AEs that are comparable with anti-PD-1/PD-L1 monotherapy use in advanced HCC (14% in KEYNOTE-394 for pembrolizumab, 15% in RATIONALE-208 for tislelizumab, and 6.4% in HIMALAYA for durvalumab; refs. 24–26). Within our study, particular scrutiny was placed on hepatic TRAEs as events of clinical interest in the context of this multimodal therapeutic approach. Reassuringly, serial evaluation of liver function tests demonstrated no evidence of treatment-related worsening liver dysfunction in the context of the TACE plus pembrolizumab sequential combination.

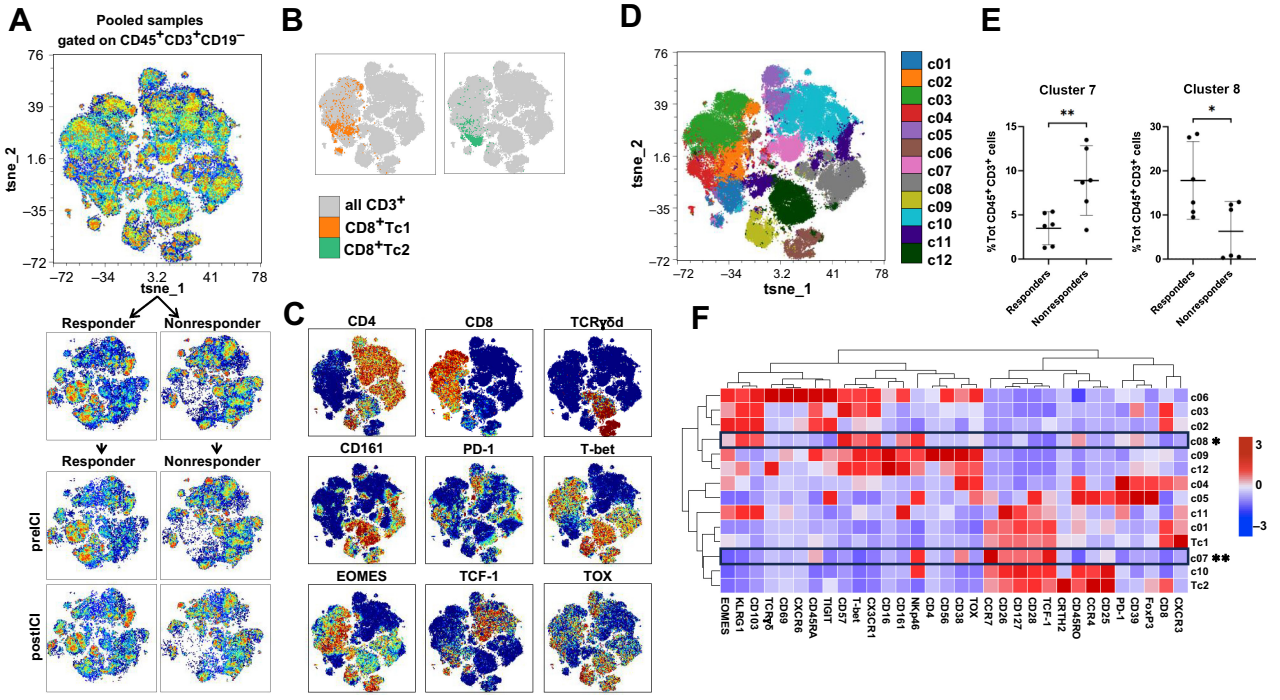

Figure 4.

A, tSNE visualization of CD45$^+$CD3$^+$CD19$^-$ T lymphocytes pooled (top), divided by response to therapy (middle), and in addition by timepoint (bottom). Each dot corresponds to a single cell. Representative data of 4 patients, subsampled up to 15,000 per sample; analysis of 157,543 cells in total. **B,** Overlay plot indicating the localization of Tc1 and Tc2 cells on the tSNE map. **C,** T-cell marker expression is visualized on the tSNE map by color heat map. **D,** T cells were clustered on the basis of their high-dimensional expression profile using FlowSOM. Clusters are visualized by the indicated colors on the tSNE map. **E,** Cluster abundance of c07 and c08 in responder and nonresponder patients. Data are represented as mean with SD and analyzed by paired *t* test. **F,** Hierarchically clustered heat map indicating mean marker expression of T-cell differentiation, activation, and exhaustion markers by each cluster and including manually gated Tc1 and Tc2 subsets as in **Fig. 3**. Expression is visualized by z-score as indicated; data were scaled per column. *, $P < 0.05$; **, $P < 0.01$.

Establishing a tolerable multimodal therapy is of paramount importance in patients with HCC. Earlier clinical experience in the combination of TACE with the VEGF inhibitor bevacizumab had shown evidence of life-threatening AEs, justifying interruption of clinical development (8). The choice of sequential introduction of pembrolizumab 30 days after TACE, justified by evidence suggesting optimal recovery of liver function tests within 4 weeks from the locoregional therapy, allowed us to optimally delineate acutely emerging toxicities from the two therapies and evaluate the relative contribution of each component of multimodal therapy to the overall treatment efficacy. To complement safety data, our analysis of patient-reported outcomes portrays substantial stability across multiple validated indices describing patients' QoL. As demonstrated in advanced HCC, QoL preservation plays an important role in the definition of an appropriate benefit/risk profile from initiation of systemic therapy (27). Our findings, although limited by small sample size, are informative to the onward clinical development of immunotherapy alongside TACE by showing that integration of PD-1 inhibition does not lead to worsening of patients' QoL: a concept that should be further tested in randomized phase III studies.

Antitumor activity of pembrolizumab following TACE appeared encouraging in our study, with over 93% of patients remaining progression-free 12 weeks after treatment and for a median duration of 10.3 months. Despite the lack of a control arm, patients achieving a response to the TACE plus pembrolizumab combination achieved durable responses, lasting for a median interval of 7.3 months. By the time of data cutoff, the median OS of our cohort was 33.9 months. Whether sequential exposure to pembrolizumab following TACE may lead to a significant survival advantage in patients with intermediate-stage HCC is a research question beyond the scope of our study. However, the OS estimates reached in our study population are encouraging and compare favorably with recently published case series of patients treated with locoregional therapy (28), further strengthening the case for future research in this segment of the HCC population. Recently, the EMERALD-1 trial has demonstrated durvalumab plus bevacizumab to improve PFS after 16 weeks of TACE + durvalumab concomitant therapy, with no benefit demonstrated from the addition durvalumab monotherapy over placebo (29). While OS data from EMERALD-1 are eagerly awaited, the PFS and OS figures emerging from our study are provocative in suggesting that a proportion of patients may derive benefit from TACE plus PD-1 monotherapy without suffering excessive AEs. Whether concomitant versus sequential immunotherapy is preferred in intermediate-stage HCC is unknown and reporting of the multiple phase III studies in this field will provide clarity as to the best treatment schedule and choice of agents in this field (30).

Understanding the mechanism of action of PD-1 inhibitors in HCC is an area of high unmet need (31), especially given the lack of predictive value for standard biomarker such as PD-L1 immunostaining (32) or tumor mutational burden in HCC (33).

In this study, phenotypic characterization of the tumoral immune infiltrate in a subset of patients with pretreatment tumor biopsies available for analysis shows evidence of an association between gene

signatures reflective of tumor cell adhesion, matrix remodeling, and immune regulation and response to TACE plus pembrolizumab. Among the noted upregulation of selected acute phase reactants such as *LBP* and *FN1* in responders, we found evidence of *SPP1* overexpression, an adverse prognostic marker in HCC also known as osteopontin, which contributes to shape an immune tolerogenic microenvironment in HCC (34) through myeloid cell/macrophage polarization (35) and adversely influences immunotherapy response (36). The positive association between baseline *SPP1* expression and response to TACE plus pembrolizumab is particularly interesting as it resonates with retrospective evidence suggesting improved outcomes from TACE in patients harboring a proinflammatory tumor microenvironment (11). Whether TACE plus pembrolizumab efficiently disrupt the myeloid-enriched "tumor immune barrier" associated with immunotherapy, resistance (34) should be the focus of pairwise comparison of pre-TACE biopsy material obtained prospectively in randomized cohorts with or without immunotherapy exposure.

Data-driven high-dimensional analysis further identified a Th1-like CD4 T-cell subset that was positively associated with response to treatment, while early differentiated memory $CD4^+$ T-cell subset was negatively associated with response. Interestingly, the difference in T-cell subsets was observed prior to ICI commencement, while no significant change induced by TACE was identified.

Of note, a pre-existing CD8 T-cell response is considered a central prerequisite for optimal response to PD-1–based immunotherapy (37, 38). Our detailed phenotypic analysis of peripheral blood immune cells further dissected the different CD8 T-cell subsets, and we described an opposite association of Tc1 and Tc2 subsets with therapy outcome. The Tc1 subset frequency prior to ICI therapy was negatively associated with outcome. Phenotypic analysis of the Tc1 subset further revealed expression of many severe exhaustion-associated molecules, such as Tox, Eomes, and PD-1, suggesting severe exhaustion of this population. In contrast, the Tc2 subset was identified as a positive correlate of overall treatment success, with a reduced expression of exhaustion markers. Interestingly, the Tc2 subset expressed Tcf-1, and Tcf-1+ $CD8^+$ T cells were found to be associated with response to ICI in other malignancies (39).

Effective antitumor rejection relies on the complementary role of IFNγ-secreting Tc1 cells and IL4 and IL5–secreting Tc2 cells (39). IL4 and IL5 are central to both Th2 and Tc2 cell maturation and Th2/Tc2 polarization has been observed in tumor-infiltrating lymphocytes (37) in a positive correlation that mirrors the one found in responding patients to TACE plus pembrolizumab. Interestingly, previous evidence in lung cancer has shown that local antitumor therapy with cyberknife or intensity-modulated radiotherapy enhances Th2 and Tc2 responses, drawing an interesting parallel to the immunogenic effect of the TACE plus pembrolizumab observed in our study (38). While preliminary in nature, evidence of a preferential Tc2 following locoregional therapy emphasizes the role of T-cell effector function as a mechanism of action of multimodal therapy in HCC, an original finding that should constitute the basis of the biomarker development plan in larger studies of this kind.

Further insight into the disease-modulating effect of TACE plus pembrolizumab emerge from the serial analysis of circulating tumor DNA concentration across timepoints. Using targeted next-generation sequencing approach, which recapitulates the most common mutational events in HCC (21), we were able to show that the ctDNA evolution in plasma reproduces the radiological response to treatment, with a significant decrease in ctDNA levels in responders, and a significant rise in patients who did not respond to TACE plus pembrolizumab. While our analysis is limited by the lack of a tumor informed approach, longitudinal changes in the VAF of key mutational drivers of HCC highlights the potential of ctDNA as a noninvasive biomarker for the therapeutic monitoring of HCC during multimodal therapy.

Inspired by the growing interest in the gut microbiome and its perturbation as a mechanism of response to immunotherapy in HCC (40–42), our stool bacterial metagenomics and plasma metabolomics revealed significant changes in the abundance of *Clostridium* and *Alistipes* throughout treatment. *Alistipes* is an increasingly characterized genus of the *Bacteroidetes phylum* that has been associated with positive response to immunotherapy in lung cancer (43). Modification in its abundance throughout multimodal TACE plus pembrolizumab treatment may highlight a positive bidirectional modulation between the gut microbiome and local plus systemic therapy which would be important to validate as mechanism of therapeutic efficacy in larger studies. Unfortunately, the unfolding of the COVID-19 pandemic (44) prevented a systematic collection of serial stool samples in all patients, limiting our ability to explore whether measures of gut microbial diversity could scale with the extent and duration of response in our patients. However, we were able to investigate the peripheral metabolic state of patients with a comprehensive serial phenotyping. Acylcarnitines are known to be associated with cirrhosis evolution and HCC development (45) and we observed a significant decrease after TACE, as expected (46). Their increased concentration at baseline in responders could be correlated with a different nutritional status, and their association with tolerance to systemic therapy (47) should be explored further in the context of combined treatment strategies with TACE and immunotherapy.

There are limitations of this study, including limited sample size, lack of a control arm, and the deleterious impact of the COVID-19 pandemic, which made recruitment and retention of participants to this investigator-led clinical trial particularly difficult, leading to a reduction in the number of samples available for translational analyses. Despite these limitations, our study has met its primary objective, having demonstrated that the combination of TACE plus pembrolizumab is tolerable, deliverable, and characterized by preliminary but convincing evidence of efficacy in patients with intermediate-stage HCC. Our findings represent an important benchmark for the subsequent development of therapeutic combinations in intermediate-stage HCC.

Authors' Disclosures

D.J. Pinato reports personal fees from ViiV Healthcare, Bayer Healthcare, AstraZeneca, Roche, IPSEN, Lift Biosciences, MiNa Therapeutics, DaVolterra, Exact Sciences, Mursla, and Boston Scientific, as well as grants from MSD, GSK, and BMS outside the submitted work. A. D'Alessio reports personal fees from Roche, AstraZeneca, and Chugai outside the submitted work. C. Celsa reports personal fees from Roche, Ipsen, Eisai, MSD, and AstraZeneca outside the submitted work. M.R. Openshaw reports grants and non-financial support from NONACUS and personal fees from Servier outside the submitted work. H.C. Keun reports grants from Cancer Research UK Experimental Cancer Medicine Centre and NIHR Imperial Biomedical Research Centre during the conduct of the study. P.J. Ross reports personal fees from Amgen, AstraZeneca, Bayer, Eisai, Sirtex, Takeda, Boston Scientific, BMS, and Merck Serono; personal fees and other support from Servier; other support from Roche and Ipsen; and grants from Sanofi outside the submitted work. A. Cortellini reports personal fees and non-financial support from MSD, Regeneron, and Sanofi, as well as personal fees from BMS, OncoC4, AstraZeneca, and Roche outside the submitted work. B. Bengsch reports grants from German Cancer Consortium (DKTK) and Deutsche Forschungsgemeinschaft during the conduct of the study, as well as personal fees from Iomedico outside the submitted work; in addition, B. Bengsch has a patent for WO2019084493A1 issued. No disclosures were reported by the other authors.

Authors' Contributions

D.J. Pinato: Conceptualization, formal analysis, supervision, funding acquisition, investigation, methodology, writing–original draft. **A. D'Alessio:** Data curation, formal analysis, investigation, methodology. **C.A.M. Fulgenzi:** Data curation, formal analysis, investigation, methodology. **A.E. Schlaak:** Investigation. **C. Celsa:** Data curation, investigation. **S. Killmer:** Data curation. **J.M. Blanco:** Investigation. **C. Ward:** Project administration. **C.-V. Stikas:** Data curation. **M.R. Openshaw:** Data curation. **N. Acuti:** Data curation, formal analysis. **G. Nteliopoulos:** Data curation, formal analysis. **C. Balcells:** Data curation, formal analysis. **H.C. Keun:** Data curation, formal analysis. **R.D. Goldin:** Data curation, investigation. **P.J. Ross:** Data curation, investigation. **A. Cortellini:** Data curation, formal analysis. **R. Thomas:** Investigation. **A.-M. Young:** Investigation. **N. Danckert:** Investigation. **P. Tait:** Investigation. **J.R. Marchesi:** Data curation, investigation. **B. Bengsch:** Data curation, investigation. **R. Sharma:** Data curation, supervision, investigation.

Acknowledgments

This study was supported by funding from Merck Sharpe & Dohme (MSD) as an investigator-initiated study sponsored by Imperial College London. Infrastructure support was provided by the NIHR Imperial Biomedical Research Centre and the NIHR Imperial Clinical Research Facility. The views expressed are those of the author(s) and not necessarily those of the funder, the NIHR, or the Department of Health and Social Care.

D.J. Pinato is supported by grant funding from the Wellcome Trust Strategic Fund (PS3416), the Associazione Italiana per la Ricerca sul Cancro (AIRC MFAG 25697), and the Roger Williams Foundation for Liver Disease (Small Project Grant), and acknowledges grant support from the Cancer Treatment and Research Trust (CTRT), as well as infrastructural support by the Imperial Experimental Cancer Medicine Centre, Imperial College Healthcare NHS Trust Tissue Bank, and the NIHR Imperial Biomedical Research Centre. A. D'Alessio and J.R. Marchesi are supported by the National Institute for Health Research (NIHR) Imperial BRC, while A. D'Alessio is further supported by grant funding from the European Association for the Study of the Liver (2021 Andrew Burroughs Fellowship) and from Cancer Research UK (RCCPDB- Nov21/100008). C. Celsa is funded by the European Union-FESR or FSE, PON Research and Innovation 2014-2020-DM 1062/2021. B. Bengsch's research is supported by Deutsche Forschungsgemeinschaft (DFG) research grant # 520992132, 441891347 (OncoEscape), 390939984 (CIBSS), 272983813 (TRR179), 256073931 (IMPATH), and 518316185 (GMCA), and the German Cancer Consortium (DKTK). The study team would like to acknowledge Dr. Alexandros Siskos for their assistance with sample processing for metabolomics analyses, Ms. Maria Martinez for their administrative support to the study, and Ms. Naina Patel, Mrs. Nona Rama and Mr. Ignazio Puccio for their support in sample preparation for transcriptomics analyses.

Note

Supplementary data for this article are available at Clinical Cancer Research Online (http://clincancerres.aacrjournals.org/).

Received January 18, 2024; revised February 29, 2024; accepted April 3, 2024; published first April 5, 2024.

References

1. Elshaarawy O, Gomaa A, Omar H, Rewisha E, Waked I. Intermediate stage hepatocellular carcinoma: a summary review. J Hepatocell Carcinoma 2019;6:105–17.
2. Raoul JL, Forner A, Bolondi L, Cheung TT, Kloeckner R, de Baere T. Updated use of TACE for hepatocellular carcinoma treatment: how and when to use it based on clinical evidence. Cancer Treat Rev 2019;72:28–36.
3. Llovet JM, Bruix J. Systematic review of randomized trials for unresectable hepatocellular carcinoma: chemoembolization improves survival. Hepatology 2003;37:429–42.
4. Llovet JM, Real MI, Montana X, Planas R, Coll S, Aponte J, et al. Arterial embolisation or chemoembolisation versus symptomatic treatment in patients with unresectable hepatocellular carcinoma: a randomised controlled trial. Lancet 2002;359:1734–9.
5. Kudo M, Ueshima K, Ikeda M, Torimura T, Tanabe N, Aikata H, et al. Randomised, multicentre prospective trial of transarterial chemoembolisation (TACE) plus sorafenib as compared with TACE alone in patients with hepatocellular carcinoma: TACTICS trial. Gut 2020;69:1492–501.
6. Lencioni R, Llovet JM, Han G, Tak WY, Yang J, Guglielmi A, et al. Sorafenib or placebo plus TACE with doxorubicin-eluting beads for intermediate stage HCC: the SPACE trial. J Hepatol 2016;64:1090–8.
7. Meyer T, Fox R, Ma YT, Ross PJ, James MW, Sturgess R, et al. Sorafenib in combination with transarterial chemoembolisation in patients with unresectable hepatocellular carcinoma (TACE 2): a randomised placebo-controlled, double-blind, phase 3 trial. Lancet Gastroenterol Hepatol 2017;2:565–75.
8. Pinter M, Ulbrich G, Sieghart W, Kolblinger C, Reiberger T, Li S, et al. Hepatocellular carcinoma: a phase II randomized controlled double-blind trial of transarterial chemoembolization in combination with biweekly intravenous administration of bevacizumab or a placebo. Radiology 2015;277:903–12.
9. Fulgenzi CAM, Scheiner B, Korolewicz J, Stikas CV, Gennari A, Vincenzi B, et al. Efficacy and safety of frontline systemic therapy for advanced HCC: a network meta-analysis of landmark phase III trials. JHEP Rep 2023;5:100702.
10. Zerbini A, Pilli M, Penna A, Pelosi G, Schianchi C, Molinari A, et al. Radiofrequency thermal ablation of hepatocellular carcinoma liver nodules can activate and enhance tumor-specific T-cell responses. Cancer Res 2006;66:1139–46.
11. Pinato DJ, Murray SM, Forner A, Kaneko T, Fessas P, Toniutto P, et al. Trans-arterial chemoembolization as a loco-regional inducer of immunogenic cell death in hepatocellular carcinoma: implications for immunotherapy. J Immunother Cancer 2021;9:e003311.
12. Flecken T, Schmidt N, Hild S, Gostick E, Drognitz O, Zeiser R, et al. Immunodominance and functional alterations of tumor-associated antigen-specific CD8+ T-cell responses in hepatocellular carcinoma. Hepatology 2014;59:1415–26.
13. Rivoltini L, Bhoori S, Camisaschi C, Bergamaschi L, Lalli L, Frati P, et al. Y(90)-radioembolisation in hepatocellular carcinoma induces immune responses calling for early treatment with multiple checkpoint blockers. Gut 2023;72:406–7.
14. Liao Y, Wang B, Huang ZL, Shi M, Yu XJ, Zheng L, et al. Increased circulating Th17 cells after transarterial chemoembolization correlate with improved survival in stage III hepatocellular carcinoma: a prospective study. PLoS One 2013;8:e60444.
15. Hiroishi K, Eguchi J, Baba T, Shimazaki T, Ishii S, Hiraide A, et al. Strong CD8(+) T-cell responses against tumor-associated antigens prolong the recurrence-free interval after tumor treatment in patients with hepatocellular carcinoma. J Gastroenterol 2010;45:451–8.
16. Pinato DJ, Karamanakos G, Arizumi T, Adjogatse D, Kim YW, Stebbing J, et al. Dynamic changes of the inflammation-based index predict mortality following chemoembolisation for hepatocellular carcinoma: a prospective study. Aliment Pharmacol Ther 2014;40:1270–81.
17. Fu J, Xu D, Liu Z, Shi M, Zhao P, Fu B, et al. Increased regulatory T cells correlate with CD8 T-cell impairment and poor survival in hepatocellular carcinoma patients. Gastroenterology 2007;132:2328–39.
18. Fessas P, Scheiner B, D'Alessio A, CA MF, Korolewicz J, Ward C, et al. PETAL protocol: a phase Ib study of pembrolizumab after transarterial chemoembolization in hepatocellular carcinoma. Future Oncol 2023;19:499–507.
19. Heimbach JK, Kulik LM, Finn RS, Sirlin CB, Abecassis MM, Roberts LR, et al. AASLD guidelines for the treatment of hepatocellular carcinoma. Hepatology 2018;67:358–80.
20. Blazeby JM, Currie E, Zee BC, Chie WC, Poon RT, Garden OJ. Development of a questionnaire module to supplement the EORTC QLQ-C30 to assess quality of life in patients with hepatocellular carcinoma, the EORTC QLQ-HCC18. Eur J Cancer 2004;40:2439–44.
21. Howell J, Atkinson SR, Pinato DJ, Knapp S, Ward C, Minisini R, et al. Identification of mutations in circulating cell-free tumour DNA as a biomarker in hepatocellular carcinoma. Eur J Cancer 2019;116:56–66.
22. Pol J, Vacchelli E, Aranda F, Castoldi F, Eggermont A, Cremer I, et al. Trial Watch: immunogenic cell death inducers for anticancer chemotherapy. Oncoimmunology 2015;4:e1008866.
23. Foerster F, Galle PR. The current landscape of clinical trials for systemic treatment of HCC. Cancers 2021;13:1962.

24. Ren Z, Ducreux M, Abou-Alfa GK, Merle P, Fang W, Edeline J, et al. Tislelizumab in patients with previously treated advanced hepatocellular carcinoma (RATIONALE-208): a multicenter, non-randomized, open-label, phase 2 trial. Liver Cancer 2023;12:72–84.
25. Qin S, Chen Z, Fang W, Ren Z, Xu R, Ryoo BY, et al. Pembrolizumab versus placebo as second-line therapy in patients from Asia with advanced hepatocellular carcinoma: a randomized, double-blind, phase III trial. J Clin Oncol 2023; 41:1434–43.
26. Abou-Alfa GK, Lau G, Kudo M, Chan SL, Kelley RK, Furuse J, et al. Tremelimumab plus durvalumab in unresectable hepatocellular carcinoma. NEJM Evid 2022;1:EVIDoa2100070.
27. Galle PR, Finn RS, Qin S, Ikeda M, Zhu AX, Kim TY, et al. Patient-reported outcomes with atezolizumab plus bevacizumab versus sorafenib in patients with unresectable hepatocellular carcinoma (IMbrave150): an open-label, randomised, phase 3 trial. Lancet Oncol 2021;22:991–1001.
28. Han G, Berhane S, Toyoda H, Bettinger D, Elshaarawy O, Chan AWH, et al. Prediction of survival among patients receiving transarterial chemoembolization for hepatocellular carcinoma: a response-based approach. Hepatology 2020;72: 198–212.
29. Lencioni R, Kudo M, Erinjeri J, Qin S, Ren Z, Chan S, et al. EMERALD-1: a phase 3, randomized, placebo-controlled study of transarterial chemoembolization combined with durvalumab with or without bevacizumab in participants with unresectable hepatocellular carcinoma eligible for embolization. J Clin Oncol 42: 3s, 2024 (suupl; abstr LBA432).
30. Fulgenzi CAM, D'Alessio A, Ogunbiyi O, Demirtas CO, Gennari A, Cortellini A, et al. Novel immunotherapy combinations in clinical trials for hepatocellular carcinoma: will they shape the future treatment landscape? Expert Opin Investig Drugs 2022;31:681–91.
31. Muhammed A, D'Alessio A, Enica A, Talbot T, Fulgenzi CAM, Nteliopoulos G, et al. Predictive biomarkers of response to immune checkpoint inhibitors in hepatocellular carcinoma. Expert Rev Mol Diagn 2022;22:253–64.
32. Pinato DJ, Mauri FA, Spina P, Cain O, Siddique A, Goldin R, et al. Clinical implications of heterogeneity in PD-L1 immunohistochemical detection in hepatocellular carcinoma: the Blueprint-HCC study. Br J Cancer 2019;120: 1033–6.
33. Wong CN, Fessas P, Dominy K, Mauri FA, Kaneko T, Parcq PD, et al. Qualification of tumour mutational burden by targeted next-generation sequencing as a biomarker in hepatocellular carcinoma. Liver Int 2021;41:192–203.
34. Liu Y, Xun Z, Ma K, Liang S, Li X, Zhou S, et al. Identification of a tumour immune barrier in the HCC microenvironment that determines the efficacy of immunotherapy. J Hepatol 2023;78:770–82.
35. Liu L, Zhang R, Deng J, Dai X, Zhu X, Fu Q, et al. Construction of TME and identification of crosstalk between malignant cells and macrophages by SPP1 in hepatocellular carcinoma. Cancer Immunol Immunother 2022;71: 121–36.
36. Yamauchi R, Ito T, Yoshio S, Yamamoto T, Mizuno K, Ishigami M, et al. Serum osteopontin predicts the response to atezolizumab plus bevacizumab in patients with hepatocellular carcinoma. J Gastroenterol 2023;58: 565–74.
37. Hegde PS, Karanikas V, Evers S. The where, the when, and the how of immune monitoring for cancer immunotherapies in the era of checkpoint inhibition. Clin Cancer Res 2016;22:1865–74.
38. Huang AC, Postow MA, Orlowski RJ, Mick R, Bengsch B, Manne S, et al. T-cell invigoration to tumour burden ratio associated with anti-PD-1 response. Nature 2017;545:60–5.
39. Miller BC, Sen DR, Al Abosy R, Bi K, Virkud YV, LaFleur MW, et al. Subsets of exhausted CD8(+) T cells differentially mediate tumor control and respond to checkpoint blockade. Nat Immunol 2019;20:326–36.
40. Myojin Y, Greten TF. The microbiome and liver cancer. Cancer J 2023;29:57–60.
41. Pinato DJ, Li X, Mishra-Kalyani P, D'Alessio A, Fulgenzi CAM, Scheiner B, et al. Association between antibiotics and adverse oncological outcomes in patients receiving targeted or immune-based therapy for hepatocellular carcinoma. JHEP Rep 2023;5:100747.
42. Fessas P, Naeem M, Pinter M, Marron TU, Szafron D, Balcar L, et al. Early antibiotic exposure is not detrimental to therapeutic effect from immunotherapy in hepatocellular carcinoma. Liver Cancer 2021;10:583–92.
43. Jin Y, Dong H, Xia L, Yang Y, Zhu Y, Shen Y, et al. The diversity of gut microbiome is associated with favorable responses to anti-programmed death 1 immunotherapy in chinese patients with NSCLC. J Thorac Oncol 2019;14:1378–89.
44. Pinato DJ, Zambelli A, Aguilar-Company J, Bower M, Sng C, Salazar R, et al. Clinical portrait of the SARS-CoV-2 epidemic in European cancer patients. Cancer Discov 2020;10:1465–74.
45. Li S, Gao D, Jiang Y. Function, detection and alteration of acylcarnitine metabolism in hepatocellular carcinoma. Metabolites 2019;9:36.
46. Iwasa M, Sugimoto R, Ishihara T, Sekoguchi-Fujikawa N, Yoshikawa K, Mifuji-Moroka R, et al. Usefulness of levocarnitine and/or branched-chain amino acids during invasive treatment for hepatocellular carcinoma. J Nutr Sci Vitaminol 2015;61:433–40.
47. Okubo H, Ando H, Ishizuka K, Kitagawa R, Okubo S, Saito H, et al. Carnitine insufficiency is associated with fatigue during lenvatinib treatment in patients with hepatocellular carcinoma. PLoS One 2020;15:e0229772.